AIRCRAFT WAKE VORTEX DEFORMATION IN TURBULENT ATMOSPHERE

Ingo Hennemann
Institute of Atmospheric Physics
Deutsches Zentrum für Luft- und Raumfahrt
Münchner Str. 20, D-82234 Wessling, Germany
ingo.hennemann@dlr.de

Frank Holzäpfel
Institute of Atmospheric Physics
Deutsches Zentrum für Luft- und Raumfahrt
Münchner Str. 20, D-82234 Wessling, Germany
frank.holzaepfel@dlr.de

ABSTRACT

Large-scale distortion of aircraft wake vortices appears to play a crucial role for aircraft safety during approach and landing. Vortex distortion is investigated based on large eddy simulations of wake vortex evolution in a turbulent atmosphere. A vortex identification method is developed that can be adapted to the vortex scales of interest. Based on the identified vortex center tracks, a statistics of vortex curvature radii is established. This statistics constitutes the basis for understanding, modeling, and exploiting mitigation effects of vortex distortion on wake vortex encounters.

INTRODUCTION

As an unavoidable consequence of lift, aircraft generate counterrotating pairs of trailing vortices. The wake vortices represent a potential risk for following aircraft, so separation distances between subsequent aircraft must be adhered. These distances depend on the maximum take off weight of the aircraft and on visibility; that is under visual flight rules (VFR) separation of aircraft can be relaxed upon pilot's request. The increasing demand of capacity at busy airports requires a detailed knowledge of wake vortex behavior in order to increase the airport capacity by the introduction of wake vortex advisory systems and to keep the risk of encountering severe vortices as low as possible. Overviews of different aspects of wake vortex research areas are available in Gerz et al. (2005) and in the Final Report of WakeNet2-Europe (2006).

The decay of wake vortices is at first dominated by internal diffusion and is followed by a rapid decay phase which depends strongly on atmospheric conditions like temperature stratification and turbulence (Holzäpfel, 2003). At the same time the vortices descend below the flight path, whereas strong temperature stratification, updrafts, shear layers, or ground proximity may cause the vortices to rebound.

Field measurement data (Holzäpfel, 2006) indicate that wake vortices often live much longer than anticipated by regulations. Simulations of wake evolution during approach and landing established with a software package for risk assessment indicate that in 8% of landings aircraft approach wake vortices closer than 10 m with a non-negligible circulation above 100 m^2s^{-1} (Holzäpfel et al., 2006). This means that landing within an environment of more or less decayed wake vortices seems to be daily practice. Three facts appear substantial to explain why current procedures are safe nevertheless. First, the area of a wake vortex which may exert hazardous forces and moments is relatively small. Second, the updrafts on both sides of the vortices act as protection by deflecting the encountering aircraft away from the most hazardous vortex cores. Third, in the atmospheric boundary layer wake vortices in general do not retain a linear shape but start to distort immediately after vortex generation (see Figure 1). Vortex distortion modifies the encounter geometry and may thus reduce the impact time of adverse forces and moments such that encounters result in non-hazardous short-time interferences which can frequently be observed at busy airports. This evaluation is supported by flight simulator studies (Loucel and Crouch, 2005) that show a significant reduction of maximum bank angles experienced by aircraft that encounter wavy vortices or vortex rings.

Our hypothesis is that the current safety levels during approach and landing can be attributed to a significant extent to vortex distortion. This implies that understanding and modeling of the physics of vortex distortion appears crucial for comprehensive wake vortex advisory systems and the obligatory proof of safety.

Figure 1: Strong deformation of wake vortices in the convective boundary layer visualized by smoke (with courtesy of NASA).

In the current paper large eddy simulations of wake vortex evolution in a turbulent atmosphere are introduced. During advanced vortex decay the classical vortex structure is getting lost and is replaced by an inhomogeneous conglomerate of turbulent vortices of different sizes that still feature

global rotation on wake vortex scales. It is shown that some common vortex identification methods fail in that regime and a vortex identification method is needed that can be adapted to specified vortex scales. The developed vortex identification method is described and compared to existing approaches. Finally, a method to determine vortex curvature is introduced and the achieved results are discussed.

NUMERICAL MODEL AND INITIAL CONDITIONS

We employ the LESTUF large eddy simulation (LES) code to investigate the deformation of wake vortices as a function of ambient turbulence scenarios (Holzäpfel et al., 2002). The impact of turbulence intensity parameterized by eddy dissipation rates, different turbulence length scales, and energy spectra shall be considered in future. The code solves the Boussinesq approximated equations discretized on a staggered grid with finite differences of second order accuracy in space and time. The classical Smagorinsky closure is modified by a subgrid scale model correction (Holzäpfel, 2004) to prevent unrealistic vortex core growth rates and the reduction of peak vorticity.

To achieve a fully developed background turbulence field we used a pre-run which was initialized with an isotropic, divergence-free turbulence spectrum containing only large eddies. We allow the turbulence to freely develop until it has reached a fully non-linear state after $t = 2.5\ t_{char,Turb.}$, where the dissipation rate ϵ reaches its maximum (see Figure 2). For more details of the turbulence field design, we refer to Gerz and Holzäpfel (1999) and Gerz and Schumann (1989).

Subsequently, the loss of energy due to dissipation slightly reduces the dissipation rate, but this proceeds much slower than the decay of wake vortices, as can be seen from the ratio of characteristic times of ambient turbulence and wake vortices, respectively:

$$\frac{t_{char,Turb.}}{t_{char,Vortex}} = \frac{\mathscr{L}_0}{V_{rms}} \cdot \frac{V_{\theta,max}}{r_c} \approx 125 \cdot 5.8 \qquad (1)$$

where $\mathscr{L}_0$ denotes the initial integral length scale obtained from the energy distribution, V_{rms} is the initial mean fluctuation velocity directly connected to turbulent kinetic energy TKE ($V_{rms} = \sqrt{\frac{2}{3}E}$), $V_{\theta,max}$ depicts the maximal tangential velocity of the vortex and r_c stands for the core radius of the vortex model (Han et al., 2000). Consequently the turbulence spectrums' change can be neglected during the lifetime of a wake vortex pair.

Because the dissipation rate ϵ characterizes the distribution of turbulent kinetic energy on the length scale range of wake vortices which is susceptible to turbulent disturbances, it is the preferred parameter to parameterize wake vortex decay. Once the background flow is fully developed and the desired dissipation rate is reached, we superimpose the vortex pair at $t = 2.5\ t_{char,Turb.}$.

To achieve realistic LES the development of vortex core growth rate and circulation distribution should agree with experimental results. We employ a reference circulation with averaged circulations of radii 5 m to 15 m

$$\Gamma_{5-15} = \frac{1}{11} \sum_{r=5}^{15} \left[\int_0^r \omega dA \right] \qquad (2)$$

with $\Gamma^*_{5-15} = \Gamma_{5-15}/\Gamma_0$. For an Airbus A340-300 with constant flight attitude we estimate the initial circulation Γ_0 according to the theorem of Kutta-Joukowsky to 458 $\mathrm{m^2 s^{-1}}$. The Lamb-Oseen vortex

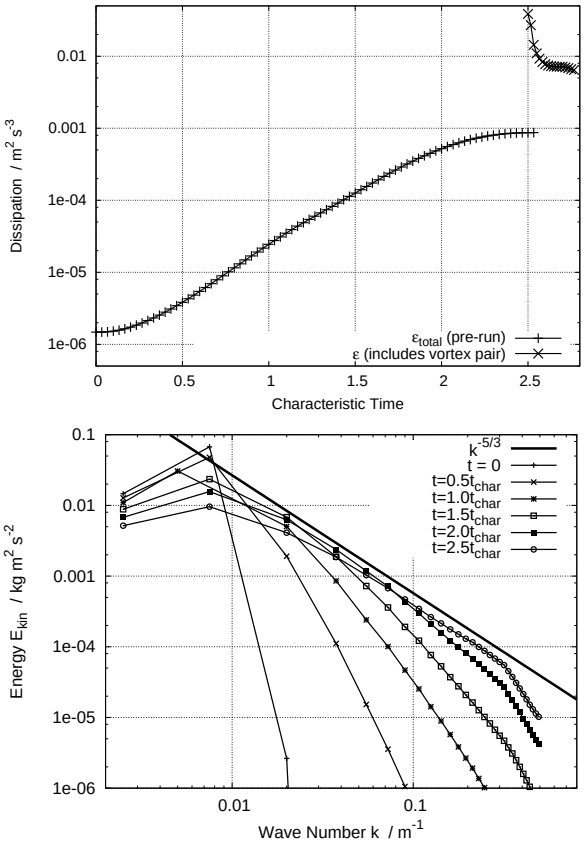

Figure 2: Temporal development of dissipation rate and spectrum during pre-run. At $t = 2.5\ t_{char,Turb.}$, the vortex pair is superimposed.

$$v_\theta = \frac{\Gamma_0}{2\pi r} \left(1 - e^{-1.2526 \left(\frac{r}{r_c}\right)^2} \right) \qquad (3)$$

shows the best results in numerical simulations, although initially other models look more realistic. The simulation domain is 400 x 256 x 256 $\mathrm{m^3}$. According to Crow (1970) vortex pairs mutually induce sinusoidal instabilities where the wave length of the dominant instability is 8.6 times the initial vortex spacing b_0 (= 47 m for an A340-300). b_0 is directly related to the span width B via the spanwise load factor s, defined as:

$$s = \frac{2}{B} \int_0^{\frac{B}{2}} \frac{\Gamma(y)}{\Gamma_0} dy \qquad (4)$$

For ellipically loaded wings s equals $\pi/4$, which is appropriate for most commercial aircraft. The domain length of 400 m guarantees that this instability mode can develop within one domain. In order to compare vortex ages of different aircraft and flight configurations, a reference time scale t_0 is introduced. Using the initial vortex descent speed w_0, it is defined as

$$t_0 = \frac{b_0}{w_0} = 2\pi \frac{b_0^2}{\Gamma_0} \qquad (5)$$

and characterizes the time a vortex pair needs to descend the distance b_0. All vortex ages are given in normalized time $t^* = \mathrm{t}/\mathrm{t}_0$. To avoid effects of anisotropic spatial resolution

on vortex curvature the simulations are highly resolved in all directions by 1 m meshes.

VORTEX IDENTIFICATION METHODS

Vortex detection and identification is of general interest in fluid mechanics. Still no universally valid definition of a vortex exists. The difficulties are on one hand related to the discrimination of shear and curvature vorticity and on the other hand to the requirement that the vortex definition should be Galilean invariant, i.e. independent from translational motions. (Banks and Singer, 1994, Haller, 2005, Holzäpfel, 2004, Spalart and Shur, 1997)

In the following we consider four options for vortex detection. First we simply employ the magnitude of the vorticity vector $|\vec{\omega}|$. But vorticity also developes in shear flows (e.g. Couette flow), which may adulterate vortex identification. One approach to distinguish between shear and curvature vorticity is suggested by Jeong and Hussain (1995). They determine the Eigenvalues of the matrix A

$$A_{ij} = S_{ij}^2 + \Omega_{ij}^2 \tag{6}$$

with $S_{ij} = \frac{1}{2}\left(\frac{\partial u_i}{\partial x_j} + \frac{\partial u_j}{\partial x_i}\right)$ and $\Omega_{ij} = \frac{1}{2}\left(\frac{\partial u_i}{\partial x_j} - \frac{\partial u_j}{\partial x_i}\right)$ and employ the (negative) second Eigenvalue λ_2 as a reliable mean to filter out shear vorticity.

Third, global rotation of any volume in fluid flow causes centrifugal forces which are balanced by pressure gradient forces. This gives reason to test a pressure minimum criterion as detection feature. Jeong and Hussain (1995) however claim that as soon as friction becomes dominant or perturbations like sinks or sources are included, the method can fail.

The forth method uses local curvature of streamlines, whereas every grid point produces one curvature radius

$$r_\kappa = \frac{|\vec{v}^2|}{|\vec{a}_n|} \tag{7}$$

from which a corresponding center of curvature can be derived (Hirsch, 1995).

In Eq. 7, r_κ is the radius of curvature and $\vec{a}_n$ the acceleration towards the curvature center (normal to $\vec{v}$). $\vec{a}_n$ can be derived from

$$\vec{a}_n = \vec{a} - \vec{v}(\vec{a}\cdot\vec{v})/|\vec{v}^2| \tag{8}$$

where $\vec{a}$ denotes the advective acceleration vector

$$\vec{a} = (\vec{v}\cdot\nabla)\vec{v} \tag{9}$$

Finally, the center of curvature ($\overline{CC}$) can be obtained by multiplying the radius of curvature (r_κ) with the corresponding direction and adding the product to the gridpoint for which curvature is computed.

$$\overline{CC} = \overline{gridpoint} + \frac{\vec{a}_n}{|\vec{a}_n|}\cdot r_\kappa \tag{10}$$

Now an array of curvature indicators i_κ shall be produced where high values represent regions of many curvature centers. This is done by augmenting the surrounding 8 nodes of each curvature center by the corresponding curvature. Hence, curvature operates as a weighting factor for the generation of the indicator array.

We want to introduce a concept that also allows to analyse wake vortex distortion in its final decay process statistically. The devised concept is a predictor - corrector process. From the starting point, the current vorticity vector proposes the direction where the track shall proceed a distance d (see Figure 3).

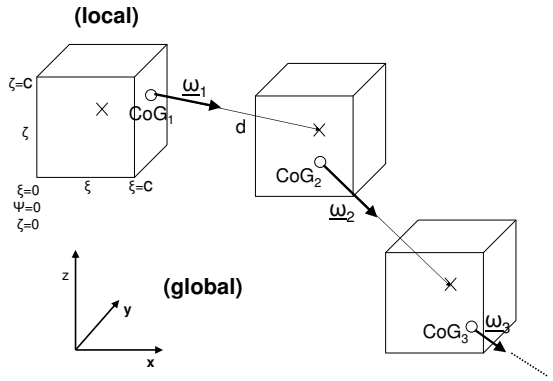

Figure 3: Predictor - corrector scheme to locate the vortex core path

Then, around the new, guessed path point (symbol x) a cubic search domain with side length c is defined, and within that search domain the criterion extremum is determined (in analogy to a center of gravity search → from now on track points will also be abbreviated CoG) to derive the position of the next vortex path point (symbol o). With that procedure all already mentioned criteria for vortex detection were tested. For pressure the mathematical formulation is (equivalent for $|\vec{\omega}|, \lambda_2, i_\kappa$):

$$\overline{x} = \frac{\int\int\int \xi\, P\, dxdydz}{\int\int\int P\, dxdydz} \tag{11}$$

$$\overline{y} = \frac{\int\int\int \psi\, P\, dxdydz}{\int\int\int P\, dxdydz} \tag{12}$$

$$\overline{z} = \frac{\int\int\int \zeta\, P\, dxdydz}{\int\int\int P\, dxdydz} \tag{13}$$

where ξ, ψ, ζ $(\in [0, c])$ are local coordinates within the cube. The method requires the criterion data to be either fully positive or fully negative, otherwise the resulting position values can be situated outside the cube.

The new vortex path point is basis for the next vorticity vector. In order to avoid misleading direction by one vorticity vector, a group of neighboring vorticity vectors is averaged.

Beside the number of participating vorticity vectors the cube size c and the distance d between two cubes can be set by the user. Simulations using criteria with frequent change of sign (like λ_2) need smaller cube lengths than smoother criteria like pressure minima. If d is too small compared to c, the center of gravity search always finds the same maximum and cannot proceed any more, if d is too large however, the track becomes imprecise. Good values turned out to be $d = 3...5$ and $c = 8...15$ mesh sizes, respectively.

Figure 3 delineates that each cube possesses its own local coordinate system (ξ, ψ, ζ) with directions equivalent to the global coordinates (x,y,z). The vector d starts at the center of gravity (CoG) of the previous cube and points towards the center of the next cube.

In order to test the quality of each criterion, a simulation in strongly turbulent environment with $\epsilon = 10^{-3}\mathrm{m}^2\mathrm{s}^{-3}$ is presented at $t^* = 4.2$ in Figure 4. At that time the vortex

tubes have already linked. The resulting vortex rings cover only half of the relevant domain length in flight direction, but increase the vortex area in lateral and vertical direction.

Each graph in Figure 4 contains iso-surfaces of the 4 criteria in similar intensities. If the vortex core track search was successful (true for P and $|\vec{\omega}|$), it is shown with the normalized circulation Γ^*_{5-15} in gray scales, too.

Only the criteria $|\vec{\omega}|$ and P allow to identify a connected vortex track without discontinuities. Methods λ_2 and i_κ produce scattered results. The pressure criterion generates smooth iso-surfaces and is best suited to find the correct vortex center track.

Figure 5 shows the same simulation at a very early time $t^* = 0.15$ with the distribution of each criterion ($|\vec{\omega}|$,λ_2,P,i_κ) per slice. At that age the four planes are considered to be equivalent. The pressure slice clearly shows the smoothest pattern, whereas absolute vorticity and curvature center are rather spotty and therefore difficult to use for the vortex identification method. λ_2 possesses a very strong gradient at the vortex core, but at later times becomes spotty, too.

Here we are not interested in small scales structures which characterize the turbulent vorticity distribution in the vortices, our purpose is to identify structures on the length scales of aircraft wake vortices.

DETERMINATION OF GLOBAL VORTEX CURVATURE

Figure 6 shows the simulated vortex tubes (represented by pressure iso-surfaces) at vortex ages of $t^* = 2.8$, $t^* = 3.0$ and $t^* = 3.15$. This sequence delineates the linking and subsequent formation of vortex rings.

For the parameterization of vortex deformation, we are interested in curvature everywhere along the vortex ring. We found that over a certain range, the vortex path lies close to one plane with a surprisingly high accuracy. That feature allows to compute that plane and proceed in 2-D. For the purpose of aircraft safety only radii on aircraft scales are important, so small curvature changes which would require to interpolate the exact vortex path are neglectable.

The algorithm searches a segment of a circle and the corresponding radius which represents all CoG of the segment best. It uses the method of least squares, where the user has the option of including the vortex track point distances to the plane or not. The search pattern employs a star shaped field with 64 search directions and up to 1000 points radially (see Figure 7).

After the optimum is determined on the coarse mesh, a finer star-shaped point pattern is created and the procedure repeats.

A first result of the curvature radii search can be seen in Figure 8. It shows the probability distribution of curvature radii for all track points of the vortex ring at $t^* = 4.2$. Here, 20 consecutive track points define one plane, and form a circle segment with minimal deviation to the circle segment. The histogram shows the distribution of radii of curvature and the corresponding RMS values at $t^* = 4.2$. Although the width of one bar is relatively small (5 m), one peak with $r_\kappa \approx 50$ m dominates the graph. Note that the x-axis scaling differs by factor 100 for core radii and RMS values, which indicates the high performance of the method.

Figure 9 shows the curvature distribution for $t^* = 3.15$ with minor peaks at $r_\kappa = 100$ m and $r_\kappa = 240$ m. In Figure 10 we show a segment of the vortex track and the fitted circle with $r_\kappa = 100$ (in the given inclined plane) which illustrates the accurate matching of the CoG track and a circle segment. Its detailed position can be seen in Figure 6 c), where the

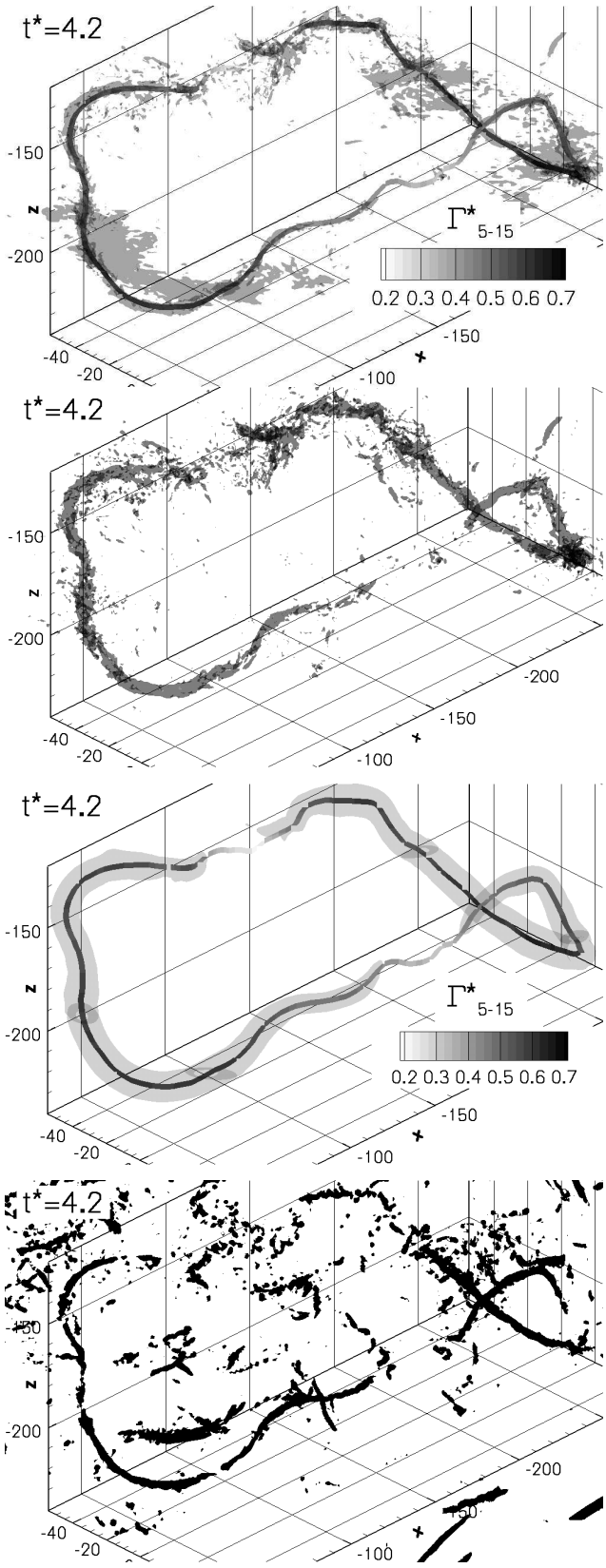

Figure 4: Iso-surfaces at $t^* = 4.2$ for corrector criteria a) absolute vorticity $|\vec{\omega}|$, b) λ_2, c) pressure P and d) curvature i_κ

cutout represents the x-values ranging from -100 to -200. The second peak is due to inflection points, where a straight line would be the best fit. However, the process checks radii

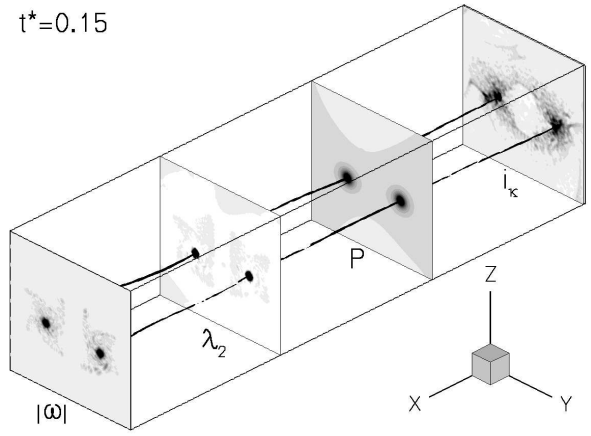

Figure 5: Iso-slices for different criteria at steady vortex tube course

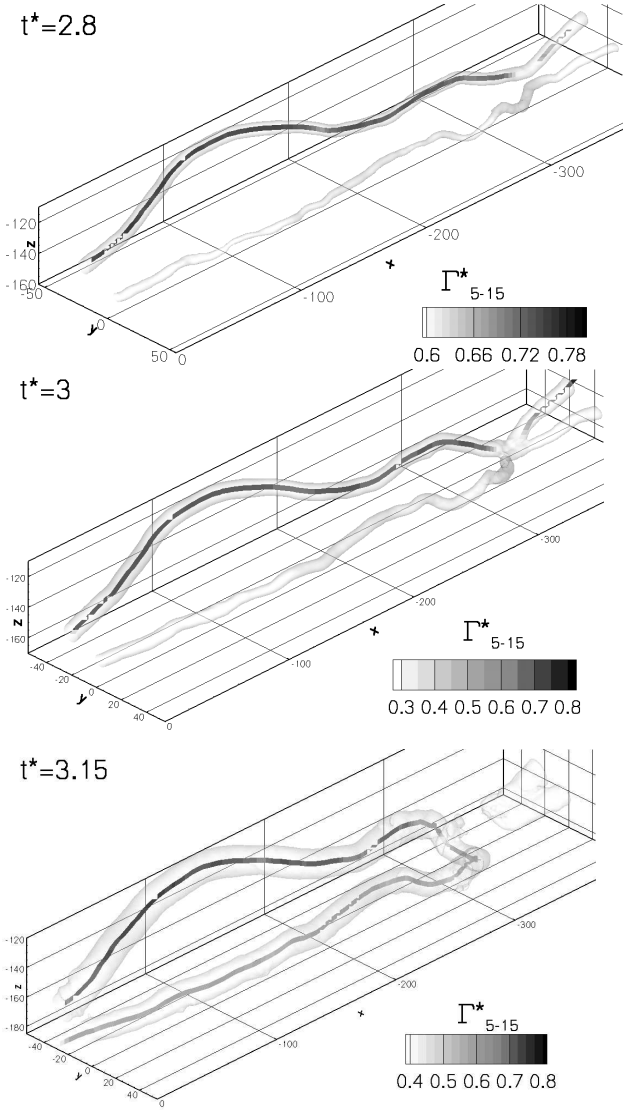

Figure 6: Ring formation at a) $t^* = 2.8$, b) $t^* = 3.0$, c) $t^* = 3.15$

up to a maximum of 240 (in this case), which is consequently found to be the best result.

The numbers given in Figure 10 represent the starting

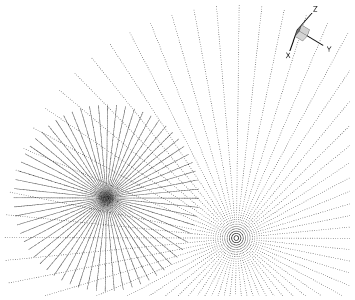

Figure 7: Search pattern to determine the best curvature radius within one plane

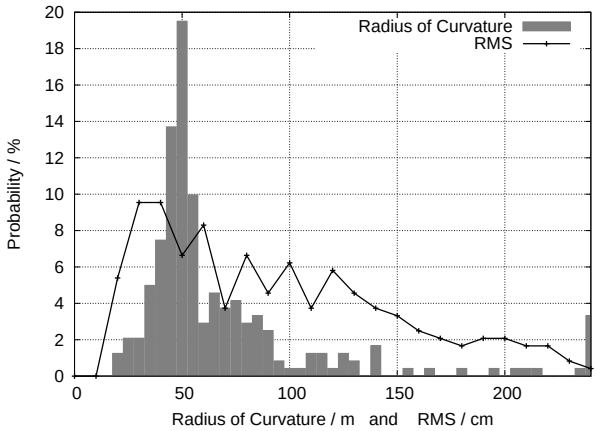

Figure 8: Probability distribution of determined curvature radii for 20 points within a given plane at $t^* = 4.2$.

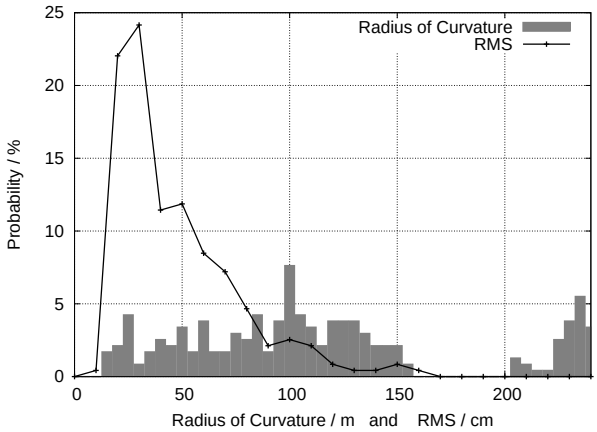

Figure 9: Probability distribution of determined curvature radii for 15 points within a given plane at $t^* = 3.15$.

number of 15 consecutive CoG for which one circle segment is searched. For example taking track points #51 to #65 yields a curvature radius of 100 m, which is shown here.

However, each time an inflection point is crossed a line would provide better results than any circle. Especially when the inflection point is situated centrally at the vortex core track, maximal curvature radii are obtained.

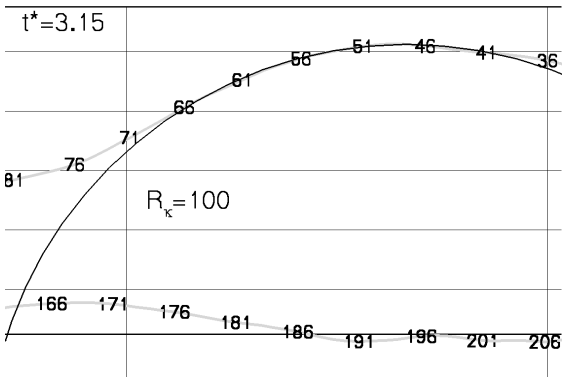

Figure 10: Output at $t^* = 3.15$ for 15 points in inclined domain, cf. Figure 6 c)

CONCLUSIONS

An algorithm is developed that allows to analyse wake vortex distortion in all spatial directions statistically. In combination with direction of vorticity, pressure is the most suitable criterion to identify the vortex core path in aircraft relevant scales. Depending on the step length between two consecutive track points, a segment including a certain number of points can be found in nearly perfect two-dimensional planes. Within these planes, that radius of curvature is searched which connects all given track points best, and all those radii of one vortex ring are summarized in a probabilistic distribution. This results in a peak radius of 50 m using 20 track points per plane at $t^* = 4.2$ in a strongly turbulent environment, with a RMS rarely exceeding 2 m. At earlier times less track points should be taken because a more distinctive variation of curvature radii occurs and RMS values decrease (nearly) proportional to the number of CoG.

Future tasks will be to automatically adapt the number of vortex track points per plane depending on the existence and position of inflection points, and also on the objectives one wants to reach. Further LES will be run with different atmospheric conditions to increase the statistic data base.

REFERENCES

Banks, D. C., Singer, B. A., 1994, "Vortex Tubes in Turbulent Flows: Identification, Representation, Reconstruction, *Proceedings of Visualization*, pp. 132-139.

Crow, S. C., 1970, "Stability Theory for a Pair of Trailing Vortices", *AIAA Journal*, Vol. 8, No. 12, pp. 2172-2179.

Gerz, T., Schumann, U., 1989, "Influence of Initial Conditions on the Development of Stratified Homogeneous Turbulent Shear Flow", Notes on Numerical Fluid Mechanics, Finite Approximations in Fluid Mechanics II, Vol. 25, *Friedr. Vieweg & Sohn.*

Gerz, T., Holzäpfel, F., 1999, "Wing-Tip Vortices, Turbulence, and the Distribution of Emissions", *AIAA Journal*, Vol. 37, No. 10, pp. 1270-1276.

Gerz, T., Holzäpfel, F., Darracq, D., 2002, "Commercial Aircraft Wake Vortices", *Progress in Aerospace Sciences*, Vol. 38, No. 3, pp. 181-208.

Gerz, T., Holzäpfel, F., Bryant, W., Kpp, F., Frech, M., Tafferner, A., Winckelmans, G., 2005, "Research Towards a Wake-vortex Advisory System for Optimal Aircraft Spacing", *Comptes Rendus Physique*, pp. 501-523.

Haller, G., 2005, "An Objective Definition of a Vortex", *Journal of Fluid Mechanics*, Vol. 525, pp. 1-26.

Han, J., Lin, Y. L., Schowalter, D. G., Arya, S. P., Proctor, F. H., 2000, "Large Eddy Simulation of Aircraft Wake Vortices Within Homogeneous Turbulence: Crow Instability" *AIAA Journal*, Vol. 38, No. 2, pp. 292-300.

Hirsch, C., 1995, "Ein Beitrag zur Wechselwirkung von Turbulenz und Drall", PhD Thesis, University of Karlsruhe.

Holzäpfel, F., Gerz, T., Baumann, R., 2001, "The Turbulent Decay of Trailing Vortex Pairs in Stably Stratified Environments", *Aerospace Science and Technology*, Vol. 5, No. 2, pp. 95-108.

Holzäpfel, F., Hofbauer, T., Gerz, T., Schumann, U., 2002, "Aircraft Wake Vortex Evolution and Decay in Idealized and Real Environments: Methodologies, Benefits and Limitations", Fluid Mechanics and its Applications, Vol. 65, Advances in LES of Complex Flows, edited by R. Friedrich, W. Rodi, *Kluwer Academic Publishers*, Dordrecht, ISBN 1-4020-0486-9, pp. 293-309.

Holzäpfel, F., 2003, "Probabilistic Two-Phase Wake Vortex Decay and Transport Model", *Journal of Aircraft*, Vol. 40, No. 2, pp. 323-331.

Holzäpfel, F., 2004, "Adjustment of Subgrid-Scale Parametrizations to Strong Streamline Curvature", *AIAA Journal*, Vol. 42, No. 7, pp. 1369-1377.

Holzäpfel, F. , Frech, M., Gerz, T., Tafferner, A., Hahn, K.-U., Schwarz, C., Joos, D., Korn, B., Lenz, H., Luckner, R., Höhne, G., 2006, "Aircraft Wake Vortex Scenarios Simulation Package", *WakeScene, 25th International Congress of the Aeronautical Sciences*, Hamburg, 12 pages.

Holzäpfel, F., 2006, "Probabilistic Two-Phase Aircraft Wake-Vortex Model: Further Development and Assessment", *Journal of Aircraft*, Vol. 43, No. 3, pp. 700-708.

Jeong, J., Hussain, F., 1995, "On the Identification of a Vortex", *Journal of Fluid Mechanics*, Vol. 285, pp. 69-94.

Loucel, R. E., Crouch, J. D., 2005, "Flight-Simulator Studies of Airplane Encounters with Perturbed Trailing Vortices", *Journal of Aircraft*, Vol. 42, No. 3, pp. 924-931.

Spalart, P.R., and Shur, M., 1997, "On the Sensitization of Turbulence Models to Rotation and Curvature", *Aerospace Science and Technology*, Vol. 1, No. 5, pp. 297-302.

Wake Vortex Research Needs for "Improved Wake Vortex Separation Ruling" and "Reduced Wake Signatures", 2006, Final Report of the Thematik Network 'WakeNet2-Europe', 6th Framework Programme, National Aerospace Laboratory, NLR-CR-2006-171, Amsterdam.